References and Notes

1. K. W. Behannon, M. H. Acuña, L. F. Burlaga, R. P. Lepping, N. F. Ness, F. M. Neubauer, *Space Sci. Rev.* **21**, 235 (1977).
2. B. U. O. Sonnerup and L. J. Cahill, *J. Geophys. Res.* **72**, 171 (1967).
3. A. J. Dessler and V. M. Vasyliunas, *Geophys. Res. Lett.* **6**, 37 (1979).
4. M. H. Acuña and N. F. Ness, *J. Geophys. Res.* **81**, 2917 (1976).
5. J. A. Gledhill, *Nature (London)* **214**, 156 (1967); C. K. Goertz, *J. Geophys. Res.* **81**, 3368 (1976).
6. L. J. Gleeson and W. I. Axford, *J. Geophys. Res.* **81**, 3403 (1976).
7. E. J. Smith, L. Davis, Jr., D. E. Jones, P. J. Coleman, Jr., D. S. Colburn, P. Dyal, C. P. Sonett, A. M. A. Frandsen, *ibid.* **79**, 3501 (1974).
8. T. G. Northrop, C. K. Goertz, M. F. Thomsen, *ibid.*, p. 3579; D. E. Jones, E. J. Smith, L. Davis, Jr., D. S. Colburn, P. J. Coleman, Jr., P. Dyal, C. P. Sonett, *Utah Acad. Sci. Arts Lett. Proc.* **51**, 153 (1974); A. Eviatar and A. I. Ershkovich, *J. Geophys. Res.* **81**, 4027 (1976); M. G. Kivelson, P. J. Coleman, Jr., L. Froidevaux, R. L. Rosenberg, *ibid.* **83**, 4823 (1978).
9. J. H. Piddington and J. F. Drake, *Nature (London)* **217**, 935 (1968); P. Goldreich and D. Lynden-Bell, *Astrophys. J.* **156**, 59 (1969).
10. S. D. Shawhan, C. K. Goertz, R. F. Hubbard, D. A. Gurnett, G. Joyce, in *The Magnetospheres of the Earth and Jupiter*, V. Formisano, Ed. (Reidel, Dordrecht, 1975); J. H. Piddington, *Moon* **17**, 373 (1977).
11. S. D. Drell, H. M. Foley, M. A. Ruderman, *J. Geophys. Res.* **70**, 3131 (1965).
12. S. Peale, P. Cassen, R. T. Reynolds, *Science* **203**, 892 (1979).
13. See, for example, R. A. Smith, in *Jupiter*, T. Gehrels, Ed. (Univ. of Arizona Press, Tucson, 1976), figure 2 and pp. 1146–1189.

14. We thank our colleagues in the Voyager project for discussions of these early results and the entire Voyager project team for the success of this experiment. We also thank G. Sisk, E. Franzgrote, and J. Tupman of the JPL for their support; C. Moyer, J. Scheifele, J. Seek, and E. Worley for contributions to the design, development, and testing at GSFC of the experiment instrumentation; and T. Carleton, P. Harrison, D. Howell, W. Mish, L. Moriarty, A. Silver, and M. Silverstein of the data analysis team for contributing to the success of the rapid magnetic fields and plasma particles data processing system. F.M.N. was supported financially by the German Ministry of Science and Technology.

20 April 1979

Plasma Observations Near Jupiter: Initial Results from Voyager 1

Abstract. *Extensive measurements of low-energy positive ions and electrons were made throughout the Jupiter encounter of Voyager 1. The bow shock and magnetopause were crossed several times at distances consistent with variations in the upstream solar wind pressure measured on Voyager 2. During the inbound pass, the number density increased by six orders of magnitude between the innermost magnetopause crossing at ~ 47 Jupiter radii and near closest approach at ~ 5 Jupiter radii; the plasma flow during this period was predominately in the direction of corotation. Marked increases in number density were observed twice per planetary rotation, near the magnetic equator. Jupiterward of the Io plasma torus, a cold, corotating plasma was observed and the energy/charge spectra show well-resolved, heavy-ion peaks at mass-to-charge ratios* A/Z* = *8, 16, 32, and 64.*

The Voyager plasma experiment is a cooperative effort by experimenters from the Massachusetts Institute of Technology, the Goddard Space Flight Center, the Jet Propulsion Laboratory, the High Altitude Observatory of the National Center for Atmospheric Research, the University of California at Los Angeles, and the Max-Planck-Institut für Aeronomie. The instrument and the experimental objectives have been described in detail (*1*) and only a brief summary is given here. The instrument consists of four Faraday cup sensors. Three of these (the A, B, and C cups) are arranged in a symmetric cluster whose axis usually points toward Earth. The axis of the fourth sensor (the D cup) is at right angles to the axis of the cluster and points roughly into the direction of corotational flow on the inbound leg of the trajectory at Jupiter; see Fig. 1. The energy range for protons and electrons is 10 to 5950 eV. The L and M modes are positive ion modes spanning this energy/charge range in 16 contiguous steps (29 percent nominal resolution in energy) and 128 contiguous steps (3.6 percent nominal resolution in energy), respectively. Positive ion measurements are made with all four sensors. Electron measurements are made only with the D sensor. The E1 mode measures electrons with energies in the range 10 to 140 eV, using 16 contiguous steps at 3.6 percent nominal resolution in energy. The E2 mode measures electrons with energies in the range 10 to 5950 eV, using 16 contiguous steps at 29 percent nominal resolution in energy. During encounter, the time required for a complete measurement cycle of four modes is 96 seconds.

In this report we describe (i) the observed crossings of the bow shock and magnetopause and the changes in their positions with external conditions, (ii) plasma properties in the dayside outer magnetosphere, (iii) properties of the plasma in the inner magnetosphere, (iv) plasma properties in the nightside outer magnetosphere, and (v) radiation effects on the performance of the instrument. The reader should bear in mind that results given here are based on a very preliminary state of the analysis. For example, the positive ion densities quoted for the inbound pass for the outer magnetosphere are based on assumptions that are only partially true, such as that the flow is corotational and supersonic and that all of the ions are protons. The first two assumptions will have to be modified and the third is certainly wrong. For this reason, no precise estimate can be given of the accuracy of the densities shown in Fig. 3. They are probably good to a factor of 5, but a final determination can only be made on the basis of a more detailed analysis. Densities quoted for the inner magnetosphere are much more accurate, for reasons which will become apparent below.

Bow shock and magnetopause crossings seen by Voyager 1 on the inbound and outbound trajectories are listed in Table 1 and shown on the trajectory plot in Fig. 1. Figure 2 shows the upstream pressure measured by Voyager 2 and extrapolated to Voyager 1, taking into account corotation delay and the different radial distances of the two spacecraft from the sun. The latter effect was the major source of delay; a typical delay time between observation at Voyager 2 and arrival at Voyager 1 was ~ 35 hours. The first bow shock crossing occurred at 85.5 Jupiter radii (R_J) at a dynamic pressure of 8×10^{-10} dyne/cm^2. Using these values of pressure and distance, P_0 and R_0, the five shock crossings observed on the inbound pass fit extremely well the relationship $P = P_0(R_0/R)^\delta$ with $\delta = 3$. This characterization agrees with that of Smith *et al.* (*2*) and confirms the conclusion of the Pioneer experimenters that Jupiter's magnetosphere is much more compressible than that of Earth. The dashed curve of Fig. 2 represents the equilibrium position of the bow shock versus pressure given by the relation above; similarly, the solid curve shows the expected position of the magnetopause, using $\delta = 3$ and a value of R_0 appropriate for the initial position of the magnetopause rather than the bow shock. The agreement with actual crossings is good.

The six magnetopause crossings observed on the inbound and outbound passes occurred at subspacecraft System III (1965) longitudes ranging from 10° to 173°; the prediction by Dessler and Vasyliunas (*3*) of a tendency for magnetopause crossings to cluster in the range 290° ± 65°, based on the presence of such a tendency in the Pioneer 10 and 11 observations, was not confirmed.

In the dayside outer magnetosphere, plasma ions exhibit a strong corotational signature on the inbound pass, as evidenced by a consistently enhanced signal in the D cup as compared to ion currents

0036-8075/79/0601-0987$00.50/0 Copyright © 1979 AAAS

in the main sensor [see Fig. 1 for the geometry of the inbound pass; see also figure 3 in (*1*)]. If one assumes that the plasma is corotating and supersonic and that the positive ions are all protons, then one can derive a "density" from the measured positive ion currents. This overall variation in positive ion number density is shown schematically in Fig. 3.

At times (but not all of the time) there are two resolved peaks in the D cup spectra, which we interpret as a narrow proton peak plus a broad heavy-ion peak consisting of a number of unresolved species. Figure 3 shows examples of such L mode spectra where the normalized curves have been obtained by dividing the measured current in a given energy channel by the energy width of the channel. Note the extreme variability of the apparent abundance ratio of heavy ions to protons. Such variations sometimes occur from one measurement to the next. The apparent proton peak does not usually appear at the energy expected for strict corotation but occurs most often at lower energies. This effect seems too large to be accounted for by a positive spacecraft charge (see below), but could be caused by a deviation of the flow from strict corotation. At other times, the positive ions are much hotter and no resolved peaks appear in the spectra (see also Fig. 3).

The population of plasma electrons observed in the outer magnetosphere during the inbound pass is characterized by a mean energy ranging from a few hundred to a few thousand electron volts. In this respect it is similar to the electron population of the plasma sheet in the terrestrial magnetosphere. The intensity of electrons increases with decreasing radial distance in a manner that is consistent with the variation of the ion density described above. In the outermost regions of the magnetosphere the intensity of electrons is relatively small and in this region relatively strong steady currents are observed in the lowest energy windows of E1. We interpret these signals as photoelectrons or secondary electrons (or both) that are trapped by a positive spacecraft potential. Similar observations have been reported in near-Earth space (*4*) and in the magnetosphere of Mercury (*5*). In agreement with this interpretation, there is a detailed inverse correlation between the observed intensity of plasma electrons and the potential of the spacecraft derived from the observed high-energy cutoff of the assumed photoelectron component. Near the magnetopause the potential of the spacecraft occasionally rose to 30 to 40 V, but at distances less than 40 R_J it was usually below the minimum value detectable (10 V).

During the first magnetospheric passage, from ~ 59 to ~ 67 R_J, sporadic increases in the intensity of kilovolt electrons were noted; at least ten events were recorded during the first ~ 12 hours spent inside the magnetosphere. The timing of these events was not related in any way to predicted crossings of the magnetic equator. In the subsequent inbound magnetospheric passage, sporadic events were also observed at distances less than 47 R_J, but

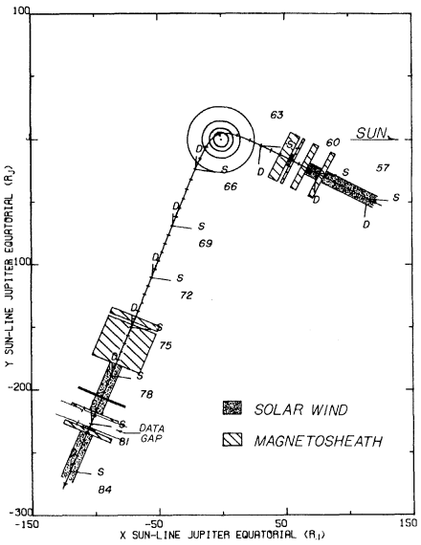

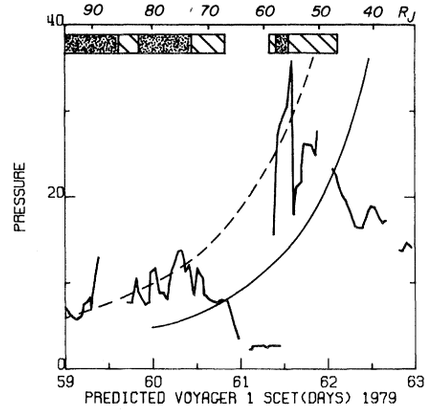

Fig. 1 (left). Voyager 1 trajectory during Jupiter encounter. The trajectory of the spacecraft and the orbits of the four Galilean satellites are seen as projected onto Jupiter's equatorial plane. Tick marks are shown every 12 hours. The projections of the look directions of the axis of symmetry of the main sensor and D cup (labeled *S* and *D*, respectively) are shown at the beginning of every third day, starting with day 57 (spacecraft event time), 26 March 1979. The look direction of the former lies almost in the plane; the foreshortening of the D cup line is indicative of its orientation out of the plane. Distances are all in units of Jovian radii (1 R_J = 71,372 km). The sections of the trajectory along which the plasma experiment measured solar wind or magnetosheath plasma are indicated. Unkeyed trajectory sections correspond to the positions at which the spacecraft was inside the magnetosphere. Fig. 2 (right). Predicted solar wind pressure at Voyager 1 based on Voyager 2 measurements. The interplanetary medium, magnetosheath, and magnetosphere are indicated as in Fig. 1; SCET is spacecraft event time. The solid and dashed smooth curves are discussed in the text. Pressure is in units of 10^{-10} dyne/cm^2.

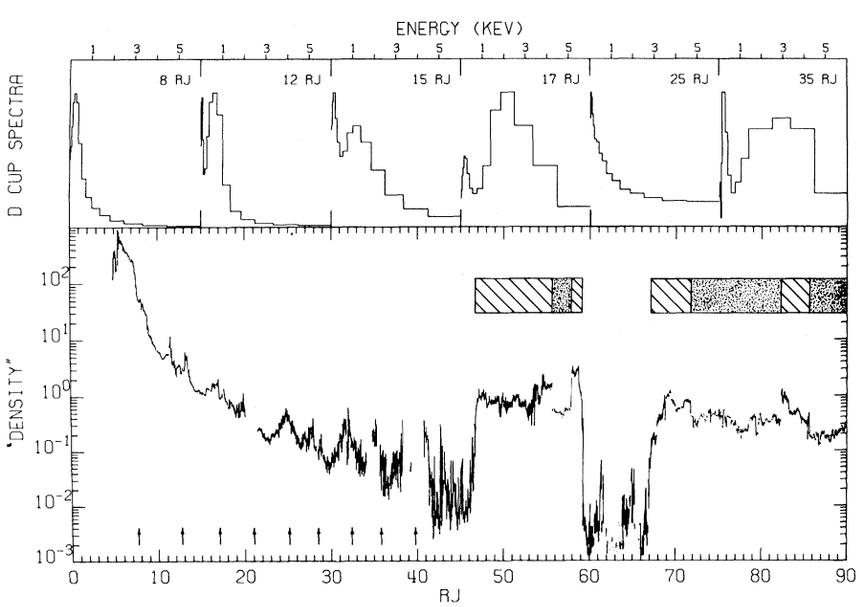

Fig. 3. Positive ion densities during the Voyager 1 inbound pass, in number per cubic centimeter. Regions of solar wind and magnetosheath flow are indicated in the same manner as in Fig. 1. Vertical arrows indicate crossings of the magnetic equator. Also shown at different distances from Jupiter are representative L mode spectra (see text) from the D cup, plotted on a linear vertical scale. The various spectra are normalized to the same maximum value.

as the distance decreased the enhanced electron fluxes occurred more often close to expected crossings of the magnetic equator.

Figure 3 clearly shows the regions of enhanced plasma density encountered at regular intervals on the inbound pass. At the times when the density is high, the magnetic field strength is low (*6*). Furthermore, the density increases occur when the spacecraft is close to the magnetic equator. Thus, it seems natural to interpret the density enhancements seen inside 35 R_J as crossings of the spacecraft through a thin plasma sheet or current sheet. The sheet rotates with the planet and moves up and down relative to the Zenographic equator. Such a current sheet was inferred by Smith *et al.* (*7*) from the Pioneer 10 and 11 measurements. In Fig. 4 we show a detailed view of one of the inbound current sheet crossings (other crossings on both the inbound and the outbound pass are similar in character). The magnetic field strength (*6*) decreases from 30 to 12 γ when the electron density increases from 0.2 to 0.9 cm^{-3}. We also show the variation of the nominal ion density during this plasma sheet crossing. Particle densities peak at the time of minimum magnetic field strength and it seems reasonable that the magnetic field depression is due to the diamagnetic effect of plasma in the plasma sheet. In that case the decrease of magnetic field pressure $B^2/8\pi$ should be balanced by a corresponding increase in particle pressure. Based on a preliminary analysis, the observed low-energy ion plasma pressure at the center of the sheet contributes substantially to this pressure balance but the electron pressure does not.

Table 1. Bow shock (S) and magnetosphere (M) boundaries observed by the Voyager plasma experiment.

Boundary	Spacecraft event time: DOY*	Spacecraft event time: Hours, minutes	Distance (R_J)	System III longitude
	Inbound pass			
S	59	1434	85.7	87°
S	59	1952	82.2	286°
S	60	1226	71.7	164°
M	60	1943	67.1	66°
M	61	0755	59.1	149°
S	61	0950	57.8	222°
S	61	1308	55.7	334°
M	62	0235	46.7	98°
	Outbound pass			
M	74	0930	158.3	98°
M	74	1657	162.8	10°
M	74	2128	165.4	173°
S	77	0704	199.2	98°
S	79	0810	227	75°
S	79	0827	227	75°
S	>80	0607	240	153°
	<80	0816		
Data gap	80	1024		
	81	0657		
S	81	0943	256	50°
S	81	1302	258	200°

*Day of year (1 January = 1).

Heavy ions are found throughout the inner magnetosphere apparently corotating with Jupiter. Within the Io plasma torus these corotating ions are quite hot; Jupiterward of the torus the plasma cools extremely rapidly. The differences in the plasma between these two regions, hot and cold, are shown in Fig. 5. In both regions the experimental data show that the bulk motion of the plasma is strictly corotational; that is, $v_r \sim 0$ and $v_t = \omega r$, where v_r and v_t are the radial and tangential components of the plasma velocity, r is the radial distance from Jupiter, and ω is the angular velocity of Jupiter. Under these conditions, all ions at a given radius move with the same speed and the corotation acts as a velocity selector. The energy/charge scan of the plasma instrument can then separate different ionic species by their mass-to-charge ratios, A/Z^* (A is atomic mass number and Z^* is effective charge number). Thus in Fig. 5 two of the energy/charge spectra show clearly resolved peaks. The changing geometry is such that the component of the corotation vector into the A sensor is almost constant for the three spectra shown (see Table 2); consequently, peaks at the same energy per charge correspond to the same value of A/Z^*. For each spectrum the various peaks, after correction for overlap, were separately fit to a convected Maxwellian distribution function; in all cases the convection speed obtained from the fit was within 0.5 km/sec of the geometrically expected speed and typically within 0.2 km/sec (thus the spacecraft potential in this region must be small). Consequently, the accuracy in A/Z^* is better than ± 2 percent for these spectra. The density and temperature found from the fits are tabulated in Table 3; absolute densities are

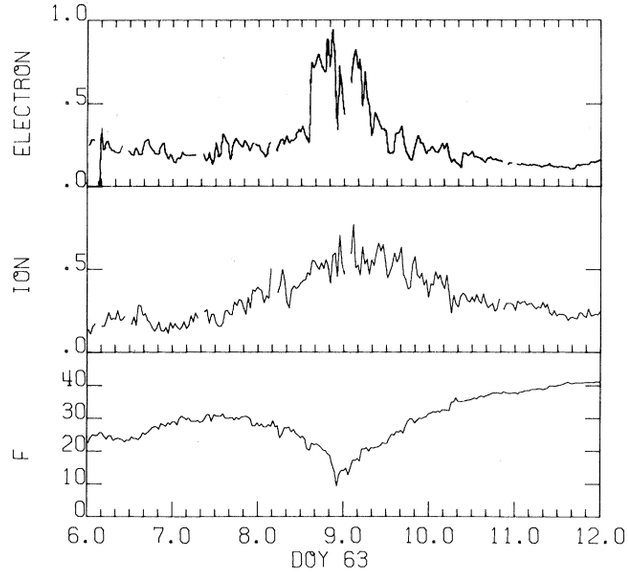

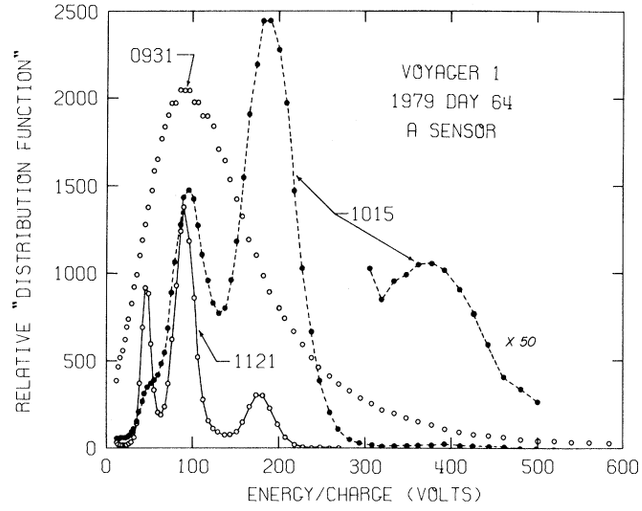

Fig. 4 (left). Plasma and magnetic field parameters for the current sheet crossing near 25 R_J inbound. Shown are electron densities (number per cubic centimeter) derived from a fit to an isotropic Maxwellian, the nominal ion densities, and the field strength F (nanoteslas). Fig. 5 (right). Comparison of the distribution function of positive ions within the Io plasma torus (0931) and at two points in the cold plasma region Jupiterward of the torus. Each curve is labeled with the spacecraft event time in hours and minutes UTC (coordinated universal time). The distribution function is plotted on a linear scale and is computed from the A sensor data of selected M mode spectra, assuming all ions are protons. The energy/charge scale is linear to 600 V, although the instrument scans to 6 kV.

Table 2. Input data for composition analysis.

Time, DOY 64	0931	1015	1121
Distance, R_J	5.63	5.30	4.96
Corotation speed relative to spacecraft, km/sec	46.5	40.5	34.3
Speed into A sensor, km/sec	32.8	33.7	33.2

good to 10 percent, relative densities to 3 percent, and temperatures to 25 percent.

The spectral peaks in Fig. 5 and Table 3 cannot be identified in an unambiguous way from the plasma data alone. However, some possibilities seem more likely on physical grounds. Since no peak is observed for values of A/Z^* between 8 and 16, the $A/Z^* = 8$ peak is almost certainly O^{2+} or a higher charge state of a heavier species. A possibility is S^{4+}, but that implies the presence of S^{3+}, which is not observed; similar arguments hold for Mg^{3+}. The $A/Z^* = 32$ peak is probably S^+. The $A/Z^* = 16$ peak is either O^+ or S^{2+}; however, in the cool region the kinetic temperatures of O^{2+}, O^+, and S^+ are the same, whereas S^{2+} is about twice as hot. Consequently, assuming thermal equilibrium, the $A/Z^* = 16$ peak in the cool region is probably mainly O^+. The peak at $A/Z^* = 64$ is unidentified but certainly real. There is no spectral evidence for N, Ne, Na, Mg, or Si, a rough limit on the density in each case being between about 1/30 and 1/10 of the appropriate neighboring peak.

The relative abundances, densities, and temperatures of the ionic species observed in the cool plasma region vary systematically with time. For example, the S/O ratio is clearly different at 1015 and 1121.

Within the torus the plasma is too hot to permit separation of closely spaced ionic species; equal amounts of S^+ and S^{2+} would, however, be resolved. This situation is illustrated by the spectrum at 0931. The peak at $A/Z^* = 16$ could be either O^+ or S^{2+}. Independent of that identification, the most probable thermal speed is ~ 16 km/sec, significantly less than that expected from the pickup speed for ions of ~ 64 km/sec. This lower speed is consistent with the cooling inferred from the large intensity of ultraviolet radiation observed by the ultraviolet spectrometer (*8*). Furthermore, the temperature is high enough so that S^{2+} is favored over S^+ and no emission characteristic of S^+ should be observable from the torus.

The inner boundary of the hot torus is well defined and the exit and entry locations are consistent with L shell control of the boundary between the hot and cold regions. A noteworthy feature is the change from S^{2+} in the torus to S^+ in the cool region.

An important unanswered question concerns the total positive ion and electron densities. Because of the small corotation velocity near 5 R_J, protons and alpha particles fall outside the range of the instrument. Thus, although an electron number density can be inferred from the observations of ions (see Table 3), it does not include contributions from ionic species with $A/Z^* \lesssim 6$. However, estimates of the total electron density in this region are available from the planetary radio astronomy and the plasma wave experiments. Using these data, it should be possible to estimate the number density of light ions that were not measured by the plasma experiment.

In the nightside outer magnetosphere, the low-energy ion and electron intensities varied regularly with distance. From day 65 until day 69—that is, from about 20 R_J to 85 R_J—the intensities peaked twice per planetary rotation. Figure 6 shows the System III (1965) longitudes at which the E2 response peaks as a function of distance from Jupiter. If the plasma were confined to the rigid equatorial plane of a magnetic dipole, the peaks should lie along the lines denoted by R. Clearly, there is a considerable lag between these predicted peaks and the observed locations. Such a lag was also observed on the Pioneer 10 outbound

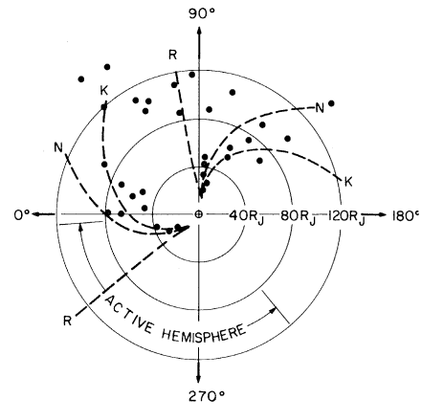

Fig. 6. System III (1965) longitudes at which the E2 response peaks on the outbound trajectory, as a function of distance from Jupiter.

pass and has been explained by Northrop *et al.* (*9*) and Kivelson *et al.* (*10*) as a result of the finite propagation time of the wave that transmits the information about the rocking magnetic dipole to the distant parts of the magnetosphere. Curves N and K in Fig. 6 indicate the expected positions according to the models of Northrop *et al.* and Kivelson *et al.*, respectively. The observed peaks lie closer to the Kivelson *et al.* predictions, although there is a systematic deviation of observed positions from the curves labeled K, in that the two peaks per rotation period occur closer together than anticipated.

In the models of Kivelson *et al.* and Northrop *et al.* the current sheet reaches a maximum latitude of 9.6° once every planetary rotation; that is, the current sheet follows the motion of the rigid magnetic equatorial plane with a certain time delay, which increases with radial distance. Since the spacecraft latitude is about 5°, the current sheet in these models should sweep across it twice per rotation period. If the maximum latitude λ_m of the current sheet is smaller than 9.6°, the two crossings should occur closer together; in the limit $\lambda_m = 5°$ the current sheet should only graze the spacecraft once per rotation period, and if $\lambda_m < 5°$ the current sheet never reaches the spacecraft. The peaks in "plasma density" should then be ill-defined and occur between the two curves labeled K. Beyond 85 R_J this appears to be the case. We would expect, on the basis of this model, that the peaks inside 85 R_J correspond to actual crossings of the current sheet (that is, $\lambda_m > 5°$) and that the magnetic field should change direction from *away* to *toward* the planet or vice versa when the magnitude is low. Most of the peaks outside 85 R_J should coincide with times when the magnetic field magnitude

Table 3. Summary of composition analysis.

A/Z^*	Possible ionic species	0931 Density (cm^{-3})	0931 Temperature (10^3 K)	1015 Density (cm^{-3})	1015 Temperature (10^3 K)	1121 Density (cm^{-3})	1121 Temperature (10^3 K)
8	O^{2+}			30	35	47	9.7
16	S^{2+}	1023	490	247	53	126	17
	O^+	2046	250	494	27	254	8.5
32	S^+			1150	25	134	9.5
64	S_2^+, SO_2^+, Zn^+			23	77		
>8 (N_e)		2046		1730		435	

decreases without a large change in direction. Comparison with the magnetometer data is necessary to confirm this interpretation. The fact that $\lambda_m < 9.6°$ indicates that the current sheet is distorted away from the magnetic equator toward the rotational equator in the way suggested by Smith *et al.* (*11*). However, inside 85 R_J the distortion must be small because the peaks are well separated in time. Beyond 85 R_J the current sheet apparently seldom moves up to latitudes in excess of 5°. This cannot be explained simply by the effects of centrifugal forces. For a centrifugally dominated magnetosphere the current sheet should reach at least a latitude of $\lambda_m = 6.4°$ (*12*) and thus cross the spacecraft twice per rotation. A more plausible explanation for the confinement of the current sheet to small latitude excursions might involve control by the solar wind; that is, formation of a tail-like structure, which could prevent the current sheet from reaching latitudes in excess of 5°.

Finally, although the current disk model is strongly supported by the observations, the existence of a once-per-rotation asymmetry in the observed region of the disk ($R < 85$ R_J), which would be indicative of significant effec ts caused by a magnetic anomaly as suggested by Dessler and Vasyliunas (*3*), cannot yet be ruled out without a closer examination of the data. However, the fact that beyond 85 R_J the peak intensities do not occur in what Dessler and Vasyliunas called the active hemisphere (the region in which the plasma source associated with the anomalies should lie) is inconsistent with the simplest form of the magnetic anomaly model unless large time delays are involved.

The high intensities of penetrating radiation belt particles found in the inner Jovian magnetosphere are potentially troublesome for a plasma experiment (*13*). The modulated grid Faraday cup, however, measures an a-c signal from which the background (which is a d-c signal) is automatically excluded. There remains a small a-c background, which is proportional to the square root of the intensity of penetrating particles. We estimated this effect to be $\sim 10^{-13}$ A at 5.0 R_J (*1*, p. 267); the background actually measured agrees with the prediction. As a result, clean ion signals were obtained directly from the Voyager plasma instrument, and the ion measurements could be immediately processed without requiring any background subtraction.

It was also anticipated by some (*14*) that the high intensities of radiation belt electrons could result in a high negative spacecraft potential, which would shift the positive ion signals to apparent high energies and possibly completely out of the range of the plasma instrument. This did not occur. Within the inner magnetosphere, significant ion currents were observed down to the lowest-energy windows of the instrument, indicating that the magnitude of the negative spacecraft potential (if any) did not exceed about 10V.

H. S. BRIDGE, J. W. BELCHER
A. J. LAZARUS, J. D. SULLIVAN
R. L. MCNUTT, F. BAGENAL
Center for Space Research and
Department of Physics,
Massachusetts Institute of Technology,
Cambridge 02139
J. D. SCUDDER
E. C. SITTLER
Laboratory for Extraterrestrial Physics,
Goddard Space Flight Center,
Greenbelt, Maryland 20771
G. L. SISCOE
Department of Atmospheric Sciences,
University of California, Los Angeles
V. M. VASYLIUNAS
C. K. GOERTZ
Max-Planck-Institut für Aeronomie,
Katlenburg-Lindau, West Germany
C. M. YEATES
Jet Propulsion Laboratory,
California Institute of Technology,
Pasadena 91103

References and Notes

1. H. S. Bridge, J. W. Belcher, R. J. Butler, A. J. Lazarus, A. M. Mavretic, J. D. Sullivan, G. L. Siscoe, V. M. Vasyliunas, *Space Sci. Rev.* **21**, 259 (1977).
2. E. J. Smith, R. W. Fillius, J. H. Wolfe, *J. Geophys. Res.* **83**, 4733 (1978).
3. A. J. Dessler and V. M. Vasyliunas, *Geophys. Res. Lett.* **6**, 37 (1979).
4. M. D. Montgomery, J. R. Asbridge, S. J. Bame, F. W. Hones, in *Photon and Particle Interactions with Surfaces in Space*, R. J. L. Grard, Ed. (Reidel, Dordrecht, 1973).
5. K. W. Ogilvie, J. D. Scudder, V. M. Vasyliunas, R. C. Hartle, G. L. Siscoe, *J. Geophys. Res.* **82**, 1807 (1977).
6. N. F. Ness, personal communication.
7. E. J. Smith, L. R. Davis, D. E. Jones, in *Jupiter*, T. Gehrels, Ed. (Univ. of Arizona Press, Tucson, 1976), p. 788.
8. L. Broadfoot, private communication.
9. T. G. Northrop, C. K. Goertz, M. F. Thomsen, *J. Geophys. Res.* **79**, 3579 (1974).
10. M. G. Kivelson, P. J. Coleman, L. Froidevaux, R. L. Rosenberg, *ibid.* **83**, 4823 (1978).
11. E. J. Smith, L. Davis, Jr., D. E. Jones, P. J. Coleman, Jr., D. S. Colburn, P. Dyal, C. P. Sonett, A. M. A Frandsen, *ibid.* **79**, 3501 (1974).
12. C. K. Goertz, *ibid.* **81**, 3368 (1976).
13. L. A. Frank, K. L. Ackerson, J. H. Wolfe, J. D. Mihalov, *ibid.*, p. 457.
14. D. A. Mendis and W. I. Axford, *Annu. Rev. Earth Planet. Sci.* **2**, 419 (1974).
15. It is impossible to make proper acknowledgement to all individuals whose efforts were essential to the success of this experiment. However, we extend special thanks to the Jet Propulsion Laboratory (JPL) project staff; to J. Binsack, R. J. Butler, C. Goodrich, G. Gordon, A. Mavretic, and Dale Ross at Massachusetts Institute of Technology; to K. Ogilvie at Goddard Space Flight Center (GSFC) and to the GSFC programming staff under W. Mish; and to the JPL data records group under J. Tupman. Finally, we express our gratitude to E. Franzgrote, our experiment representative at JPL, for his major contributions to the experiment. This research was sponsored by the National Aeronautics and Space Administration and was performed under contract 953733 to the Jet Propulsion Laboratory.

23 April 1979

Jupiter Plasma Wave Observations: An Initial Voyager 1 Overview

Abstract. *The Voyager 1 plasma wave instrument detected low-frequency radio emissions, ion acoustic waves, and electron plasma oscillations for a period of months before encountering Jupiter's bow shock. In the outer magnetosphere, measurements of trapped radio waves were used to derive an electron density profile. Near and within the Io plasma torus the instrument detected high-frequency electrostatic waves, strong whistler mode turbulence, and discrete whistlers, apparently associated with lightning. Some strong emissions in the tail region and some impulsive signals have not yet been positively identified.*

The Voyager 1 mission provided the first opportunity to examine directly wave-particle interaction phenomena within the magnetosphere of Jupiter and in the extensive region of disturbance upstream from the planet. This report contains an overview of encounter measurements from the Voyager 1 plasma wave investigation for the period starting with initial detection of Jupiter phenomena and ending a few days after closest approach. During this time, the magnetosphere was strongly affected by a dense plasma torus associated with Io (*1*) and perturbed by changing interplanetary conditions (*2*). Some interactions in the Io plasma torus resembled those found in Earth's plasmasphere. This region contained strong whistler mode turbulence (chorus, hiss, and impulsive signals that appear to be associated with lightning). Electrostatic emissions related to the electron gyrofrequency harmonics and upper hybrid resonance were also detected beyond the boundary of the torus and near the magnetic equator crossings. Radio waves trapped between the outer torus region and the dayside magnetopause (continuum radiation) allowed us to determine electron density profiles, as

0036-8075/79/0601-0991$00.50/0 Copyright © 1979 AAAS